PHYSICAL REVIEW B **82**, 020201(R) (2010)

Anisotropic atomic motion at undercooled crystal/melt interfaces

Wai-Lun Chan and Robert S. Averback
Department of Materials Science and Engineering, University of Illinois at Urbana-Champaign, Urbana, Illinois 61801, USA

Yinon Ashkenazy
Racah Institute of Physics, Hebrew University of Jerusalem, 91904 Jerusalem, Israel

(Received 11 April 2010; revised manuscript received 19 June 2010; published 22 July 2010)

Dynamics of crystal growth in pure metals is investigated as a function of undercooling using molecular dynamics computer simulations. For growth on (100) in fcc and (100) in bcc metals, we observe that the atomic mobility of atoms at the interface far exceeds that in the bulk liquid and that this difference grows with increasing undercooling. The higher mobility is associated with a small fraction of atoms undergoing long jumps. These long jumps, moreover, are anisotropic, showing enhancement along closed packed directions in the crystal. The lengths of the long jumps, however, are considerably smaller than interatomic distances. The results are interpreted using a defect model of crystallization.

DOI: 10.1103/PhysRevB.82.020201 PACS number(s): 64.70.D−, 68.08.De, 81.30.Fb, 61.25.Mv

How atoms rearrange themselves at the interface when a crystal advances into an undercooled melt remains poorly understood despite its important role in the processing of metal alloys or pure metals under extreme temperature gradients. An often employed assumption is that each atom at the melt/crystal interface hops individually and randomly between the two phases. The validity of this simple assumption, however, is becoming increasingly questionable as our understanding of the structure of the interface[1–7] and dynamics of undercooled liquids improve.[8,9] Recent simulations[10,11] and experiments[12] have shown, for example, that classical solidification models are inadequate to explain the solidification kinetics in the deeply undercooled regime. It is now recognized that a few layers of the melt neighboring the crystal inherit some "ordering" from the crystalline phase.[1–7] Theoretically, this partial ordering is found to significantly increase the crystallization velocity since atoms at the interface transform cooperatively instead of individually into the crystalline state.[4] In addition to layering of the liquid phase at solid-liquid interfaces, lateral ordering of the liquid has also been observed at heterogeneous interfaces in both experiments[1,6] and simulations.[6] For single component materials, ordering has been observed in simulations of covalently bonded materials, such as Si,[13] and a simple metallic interface, although, in the latter case, the solid atoms were kept at $T=0$.[14]

In the present work we have examined the dynamics of atomic motion in the interface of pure fcc (Ni) and bcc (Fe) metals during solidification over a wide range of temperatures, 0.8 T_m to 0.2 T_m (where T_m denotes the melting temperature). While there is a great number of past molecular dynamics (MD) simulations on this topic, most of these have considered only the macroscopic interface velocity[10,11,15,16] or the detailed structure of the interface near the melting temperature.[5] Here we focus on how the local structure affects the interface kinetics. In particular, we show that the atomic mobility in the solid-liquid interface at large undercoolings is much greater than in the bulk liquid, that the enhanced mobility is due to a few atoms undergoing large displacements, and finally that the long jumps are highly anisotropic, being strongly correlated with the close-packed directions in the relevant crystalline structure.

The simulations were performed using LAMMPS, which is a parallel MD code.[17] Ni and Fe are represented by embedded atom method potentials.[18,19] These potentials have been used widely to simulate the properties of both liquids and solids, including the kinetics and thermodynamics of solid-liquid interfaces.[15,16,20] The simulation cells, which used periodic boundary conditions, contained about 6×10^5 atoms with approximately 3×10^3 atoms per monolayer (ML) along the z direction. Solid-liquid interfaces were created in one of two methods. In one, half of the sample was heated to form a liquid near the melting temperature, this system was then relaxed for a period of ≈1 ns at the melting temperature and joined with a crystal at the same temperature. The combined system was subsequently relaxed an additional 500 ps using LAMMPS implemented Nose-Hoover temperature and pressure controls. Pressure control was applied along the z direction of the cell while holding the x and y sizes fixed at the equilibrium crystalline sizes. This allowed any excess liquid to flow and relax via cell elongation. The entire system was then quenched to a target temperature (ranging from 0.8 T_m to 0.2 T_m) at a rate of 10^{15} K ps^{-1}. Then, as the crystalline front moved, the system was again simulated using global temperature control with pressure control again activated along the z direction of the cell. In the second method, half of the system was heated to a high temperature (twice the melting temperature) for a period of 10 ps and then the whole system was brought to the target temperature with pressure control again activated along the z direction.

In both cases the interface was allowed to move ≈20 ML and reach a steady state interface velocity. Only then was the detailed kinetics studied by monitoring atom motions for a period of 10 ps. All results reported here are independent of the method used to produce the initial interface as well the temperature and pressure control parameters which were varied between 0.1 and 1 ps for the pressure and 0.05 and 0.2 ps for the temperature.

We note that heat liberated at the solid-liquid interface results in an increase of interface temperature by 20–50 K. These thermal gradients are largely artificial in the respect that the potential does not have an electronic contribution to

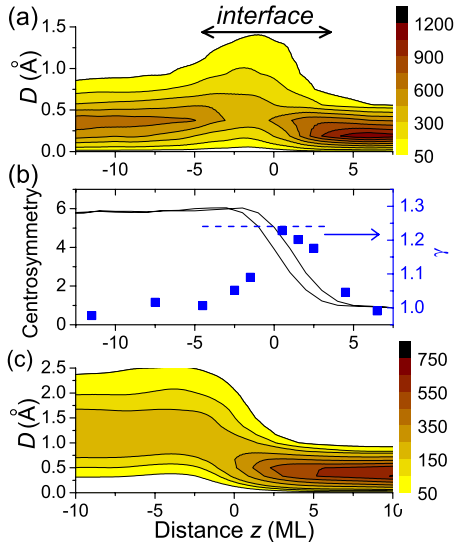

FIG. 1. (Color online) (a) The displacement of the atoms as a function of position z. The crystalline phase is on the positive z side. The gray scale is proportional to the number of atoms per unit distance that have a displacement length D. (b) The centrosymmetry (solid lines) and the anisotropy ratio γ (squares) as a function of z. The two solid lines represent the centrosymmetry at t and $t+\Delta t$. The dashed line indicates γ for the interfacial pairs (defined in the text). (c) The displacement of atoms as a function of z, for interface temperature=1490 K.

the thermal conductivity and that the whole system is thermostated (including interface atoms). While these thermal gradients can have a strong effect on interface mobility close to the melting temperature,[21] where driving forces are small, they have little effect on interface kinetics in the deeply undercooled regime reported here (see e.g., Ref. 11 and details below).

We report first on the mobility of atoms in undercooled liquid Ni near the crystal/melt interface. This is done by finding the displacement D of each atom during a fixed period Δt, i.e.,

$$D_i = |\vec{x}_i(t+\Delta t) - \vec{x}_i(t)|. \quad (1)$$

The subscript i is the atom label, and $\boldsymbol{x}$ is the position vector of the atom; Δt=1.3 ps. This time represents the time required for the crystal to advance ≈1 ML≈1.8 Å, which is the lattice spacing of the (002) plane. Figure 1(a) shows a contour plot of the numbers of atoms with a final position z and a jump distance D_i for Ni at a temperature of 660 K. The location of the interface at time, t, can be determined by plotting the average centrosymmetry factor (CSF) of atoms[22] as a function of z; this is shown as a solid line in Fig. 1(b). The two curves represent the CSF determined at t and at $t+\Delta t$. The CSF is a convenient way to distinguish the local environment of an atom since the crystalline phase has a much lower CSF than the disordered phase. From Fig. 1(b), we see that the interface extends over a thickness ≈7 ML. This thickness, in fact, represents the roughness of the crystalline interface, which can be directly observed from the image of the interface. By comparing Figs. 1(a) and 1(b), we see that the atoms near the interface have larger displacements in comparison to those in the bulk liquid or crystalline solid. Note that D remains large for 2–3 ML even though the CSF has already increased to the liquid value. This indicates that these 2–3 ML are largely disordered but that their structure and dynamics are different from those of the bulk melt. In the 2–3 ML abutting the crystalline phase, partial ordering in the z direction, similar to that reported in Ref. 5, can be observed visually from the image of the interface, although we do not show it here.

The increase in interface mobility found above at 660 K is also observed for temperatures up to ≈1200 K; it does disappear, however, at still higher temperatures (1490 K), as shown in Fig. 1(c). This occurs simply because atoms in the liquid phase become more mobile with temperature and eventually this motion outweighs the interface motion shown in Fig. 1(a). This perhaps explains why a similar enhancement in mobility was not observed in studies performed near the melting temperature.[5] In the following, we focus on the results for Ni at 660 K, although the main observations are insensitive to temperature between 300 and 1200 K.

The value of D calculated in Eq. (1) can originate from various diffusion mechanisms, e.g., relative motion between neighboring atoms, atomic vibrations, rotation of a small group of atoms in the melt, and density change of the melt during solidification. We thus consider the relative displacement of neighboring atoms during solidification, rather than total displacements, as this separates the atomic rearrangements near the interface from other motions. We thus define the relative displacement vector $\boldsymbol{R}_{ij}$

$$\vec{R}_{ij} = [\vec{x}_i(t+\Delta t) - \vec{x}_i(t)] - [\vec{x}_j(t+\Delta t) - \vec{x}_j(t)]. \quad (2)$$

The subscript j labels the nearest-neighbors (NN) atoms of atom i at time t. In order to restrict our analysis to include only relative displacements of NN and exclude next-nearest neighbors, we choose a cut-off radius of 3 Å to define NN atoms. This value is ≈10% smaller than the distance to the first minima in the pair correlation function; it neglects ≈9% of NN. The use of Eq. (2) effectively eliminates small but not insignificant density changes due to solidification. To determine $\boldsymbol{R}_{ij}$ at the interface, we examine atoms within 8 ML of the interface [represented by the arrow in Fig. 1(a)]. In order to identify the real interface atoms from these, we choose atoms that had a centrosymmetry >3.5 at t and <3.5 at $t+\Delta t$ are chosen. These atoms are the ones that changed state from a liquid to a crystalline structure within Δt. The number of atoms identified this way, corresponds to ≈1.2 ML of atoms per Δt, i.e., ≈3800 atoms. These atoms are labeled as atom i in Eq. (2). Their NN's, found at time t, are labeled as atom j. We denote pairs determined by this criterion as interfacial pairs. $\boldsymbol{R}_{ij}$ is calculated by following the positions of the interfacial atom pairs at t and $t+\Delta t$.

Figure 2 shows the probability distribution $P(R)\mathrm{d}R$ of finding a vector with magnitude R for all the interfacial pairs (the line labeled "interfacial pairs"). For comparison, the distribution for all the NN pairs in a uniform melt is shown as the black line. The distribution for atoms in the bulk melt fits well with a Gaussian, as would be expected for local random vibration of atoms. For the interfacial pairs, we fit the portion

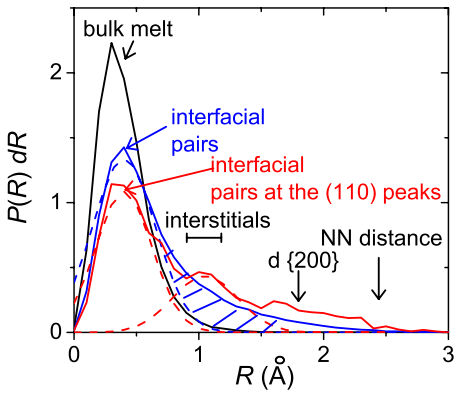

FIG. 2. (Color online) The probability distribution of the relative displacement vector ***R*** for a bulk melt, interfacial pairs, and interface pairs with ***R*** pointing to the in-plane ⟨110⟩ directions. The dashed lines are Gaussian fits to the curves. The shaded region under the curve labeled "interfacial pairs" represents the long jumps.

at small R with a Gaussian (the dashed line) and a residue at large R, the shaded region in Fig. 2. We refer to the motion represented by the shaded region as "long jumps" but bearing in mind that they are still less than one atomic distance. The shaded region accounts for ≈20% of the total number of pairs. From this result, we see that the high mobility at the interface is not simply an increase of the overall vibration amplitude as would have been suggested by the locally liberated latent heat (note the non-Gaussian distribution and only a small shift in the peak position) but rather it is due to the small portion of atoms making particularly long displacements.

We consider these interfacial pairs further by characterizing the directionality of the average jump distance. We calculate the average value of R in different directions, which can be represented by a contour plot on the surface of a unit sphere. The projections onto the x-z and x-y planes are shown in Figs. 3(a) and 3(b), respectively. Positive z points toward the crystalline phase. Distinct peaks can be observed along the close-packed ⟨110⟩ directions with the ⟨110⟩ directions parallel to the interface having particularly strong intensities. As expected, the peak pointing toward to the crystal is stronger than the peak pointing away from it. To quantify

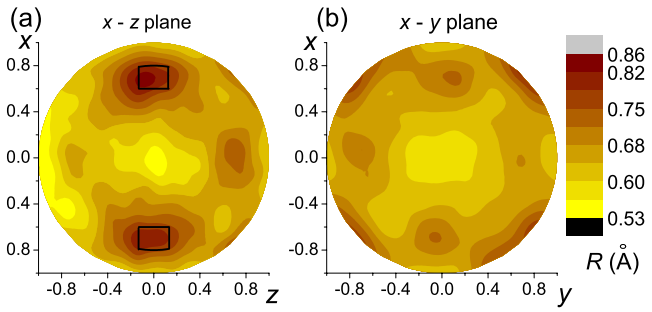

FIG. 3. (Color online) Contours plot of average R at different directions, projected onto the (a) x-z and (b) x-y plane for the Ni(001) interface at a temperature of 660 K. Positive z represents vectors pointing toward the crystal.

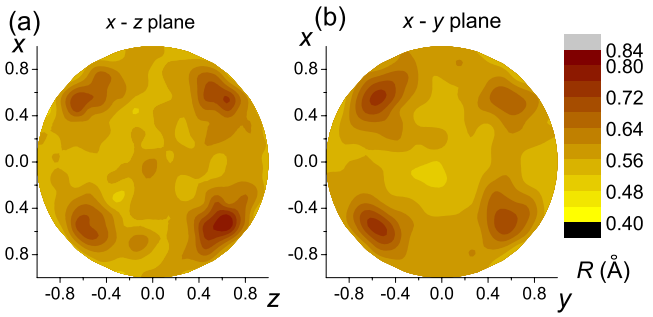

FIG. 4. (Color online) The same contour plots as Figs. 3(a) and 3(b) for bcc Fe(001) interface at 640 K.

the *directionality*, we define a ratio γ equal to the jump distance at the peaks [the squares in Fig. 3(a)] divided by the average jump distance for all pairs. For the interfacial pairs, γ equals 1.25 [shown as the dashed line in Fig. 1(b)]. We can also determine γ as a function of z. Instead of choosing pairs based on the change in centrosymmetry, we now choose pairs based on the final position of the atom i. The change in γ as a function of z is plotted in Fig. 1(b). We see that the disappearance of the directionality tracks closely with the change in centrosymmetry, thus illustrating some in-plane ordering of the liquid near the interface. We note that further from the interface, even though long jumps are still found, the directionality is lost (i.e., $\gamma \approx 1$).

We also determined $P(R)\mathrm{d}R$ for the interfacial pairs lying within these peak directions. The result is shown as the red line in Fig. 2. An excess of long jumps is found in this subset of interfacial pairs; the fraction of long jumps between 0.4 and 1 NN distances increased by ≈40% compared to that for all interfacial pairs. Noteworthy is that while the orientation of these long jumps agree with the symmetry of the crystalline interface, the jump distance is surprisingly far shorter than the NN distance. The symmetry of the jumps, therefore, cannot be a simple consequence of atoms moving from one site on the crystalline interface to another. Results similar to these for Ni are observed in BCC Fe. Using the same methods for an Fe interface at 640 K, we obtain the results shown in Fig. 4. The peaks are now found along ⟨111⟩ directions, which correspond to the close-packed directions of the bcc lattice.

Our results show that less than ≈20% of the interfacial pairs undergo long jumps. We believe that these long jumps, which are far fewer away from the interface, play an important role in the solidification process. Since the fraction of atoms making these jumps is small, each jump on average must lead to the transformation of several other atoms. This suggests that the transformation occurs via the rearrangement of a group of atoms instead of the attachment of individual atoms to the crystal. In order to characterize the nature of this rearrangement, we have examined the spatial correlation (projected onto the x-y plane) of atoms leaving the liquid and joining the crystal in the time interval, Δt, for 1 ML to crystallize. The value of the correlation function is normalized to 1 for a uniformly crystallized layer. Figure 5 illustrates that the correlation is larger than 1 for small distances. This means that groups of atoms transform from the melt to crystal with a correlation length of ≈0.5 nm. For reference, a

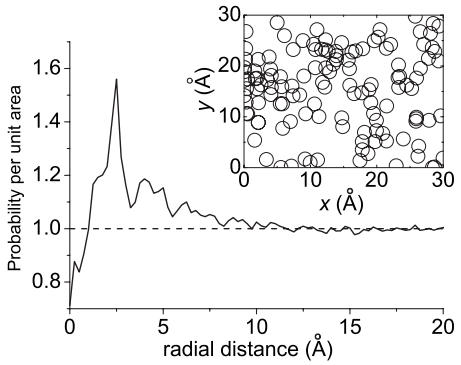

FIG. 5. The spatial correlation of atoms that will solidify in a time interval Δt where 1 ML of atoms is solidified. The x axis represents distances between atoms projected onto the x-y plane. (Inset) A projected image shows the initial positions of the solidified atoms.

projected view of the interface showing only the atoms that solidify in Δt, is included as an insert in Fig. 5. These correlations might suggest a defectlike mechanism of crystallization, whereby a defect in the ordered liquid annihilates in the interface and is accompanied by local relaxation of several neighboring interfacial liquid atoms.

We find this "defect-based" description of a liquid attractive in explaining solidification kinetics since it connects the crystal structure with the liquid structure, i.e., the solidification process is simply the annihilation of defects (e.g., interstitials) at the interface. Indeed, a recent study[10] showed that atoms in the crystal/melt interface that underwent long jumps in Fe, similar to those found here, had the distinctive structure of a dumbbell interstitialcy defect prior to joining the crystal. To compare this finding with the current result, we determine the quantity $\boldsymbol{R}_{ij}$ defined in Eq. (2) for an interstitial atom in crystalline Ni with its NN when it undergoes one jump in the crystal; an intersticialcy defect consists of two atoms sharing one lattice site. We found that six of these relative jumps are at or close to the ⟨110⟩ directions with its distance ranging from 0.9 to 1.2 Å. This distance is shown in Fig. 3 for comparison with the distribution of displacements of interface atoms. We see that our result, that many atomic displacements in the interface have the symmetry of the lattice but which have a jump distance much smaller than interatomic spacing, can indeed be explained by interstitialcy motion.

In summary, our analysis shows that the atomistic mechanisms underlying the solidification process is more complex than the simple attachment-detachment process assumed in classical solidification models and that structural order on the liquid side of the interface plays an important role. We find that ≈20% of the atoms undergo particularly long displacements in moving from the liquid to the solid, and that the directions of these jumps have a tendency to align with the underlying close-packed directions of the crystal, ⟨110⟩ for fcc Ni and ⟨111⟩ for bcc Fe. Our results also suggest that relaxations around the long jumps lead to a rearrangement of nearby atoms and crystallization.

The authors acknowledge the support by the U.S. DOE-NNSA under Grant No. DE-FG52-06NA26153 and the U.S. DOE-BES under Grant No. DE-FG02-05ER46217.

[1] S. H. Oh, Y. Kauffmann, C. Scheu, W. D. Kaplan, and M. Ruhle, Science **310**, 661 (2005).
[2] F. Spaepen, Acta Metall. **23**, 729 (1975).
[3] D. W. Oxtoby and A. D. J. Haymet, J. Chem. Phys. **76**, 6262 (1982).
[4] L. V. Mikheev and A. A. Chernov, J. Cryst. Growth **112**, 591 (1991).
[5] B. J. Jesson and P. A. Madden, J. Chem. Phys. **113**, 5935 (2000).
[6] W. D. Kaplan and Y. Kauffmann, Annu. Rev. Mater. Res. **36**, 1 (2006).
[7] Y. Mishin, M. Asta, and J. Li, Acta Mater. **58**, 1117 (2010).
[8] C. Donati, J. F. Douglas, W. Kob, S. J. Plimpton, P. H. Poole, and S. C. Glotzer, Phys. Rev. Lett. **80**, 2338 (1998); S. C. Glotzer, J. Non-Cryst. Solids **274**, 342 (2000).
[9] K. Nordlund, Y. Ashkenazy, R. S. Averback, and A. V. Granato, Europhys. Lett. **71**, 625 (2005).
[10] Y. Ashkenazy and R. S. Averback, EPL **79**, 26005 (2007).
[11] Y. Ashkenazy and R. S. Averback, Acta Mater. **58**, 524 (2010).
[12] W.-L. Chan, R. S. Averback, D. G. Cahill, and Y. Ashkenazy, Phys. Rev. Lett. **102**, 095701 (2009).
[13] D. Buta, M. Asta, and J. J. Hoyt, Phys. Rev. E **78**, 031605 (2008).
[14] A. Hashibon, J. Adler, M. W. Finnis, and W. D. Kaplan, Comput. Mater. Sci. **24**, 443 (2002).
[15] D. Y. Sun, M. Asta, and J. J. Hoyt, Phys. Rev. B **69**, 024108 (2004); **69**, 174103 (2004).
[16] D. Y. Sun, M. Asta, J. J. Hoyt, M. I. Mendelev, and D. J. Srolovitz, Phys. Rev. B **69**, 020102 (2004).
[17] S. J. Plimpton, J. Comput. Phys. **117**, 1 (1995).
[18] S. M. Foiles, M. I. Baskes, and M. S. Daw, Phys. Rev. B **33**, 7983 (1986).
[19] M. I. Mendelev, S. Han, D. J. Srolovitz, G. J. Ackland, D. Y. Sun, and M. Asta, Philos. Mag. A **83**, 3977 (2003).
[20] J. J. Hoyt, D. Olmsted, S. Jindal, M. Asta, and A. Karma, Phys. Rev. E **79**, 020601 (2009).
[21] J. Monk, Y. Yang, M. I. Mendelev, M. Asta, J. J. Hoyt, and D. Y. Sun, Model. Simul. Mater. Sci. Eng. **18**, 015004 (2010).
[22] C. L. Kelchner, S. J. Plimpton, and J. C. Hamilton, Phys. Rev. B **58**, 11085 (1998).